PHOTONICS Research

Applying a mixed light field generated from a two-level atomic ensemble to two-photon interference

Shuyu Zhou,[1,*] Shanchao Zhang,[2] Ying Wang,[3] and Yuzhu Wang[1]

[1]Key Laboratory for Quantum Optics, Shanghai Institute of Optics and Fine Mechanics, Chinese Academy of Sciences, Shanghai 201800, China
[2]Guangdong Provincial Key Laboratory of Quantum Engineering and Quantum Materials, SPTE, South China Normal University, Guangzhou 510006, China
[3]School of Mathematics and Physics, Jiangsu University of Science and Technology, Zhenjiang 212003, China
*Corresponding author: syz@siom.ac.cn

Received 23 December 2019; revised 1 March 2020; accepted 19 March 2020; posted 20 March 2020 (Doc. ID 386557); published 6 May 2020

A mixed light field generated from a two-level atomic ensemble can be used for two-photon interference. In this mixed light field, correlated paired photons generated from a four-wave mixing process provide a signal of two-photon interference, while Rayleigh scattered photons of the pump laser provide a stable reference to calibrate the normalized second-order correlation function. We demonstrate two-photon interference using the Hong–Ou–Mandel and Hanbury Brown–Twiss interferometers. A direct quantitative comparison between theoretical predictions and experimental data is performed under perturbed experimental conditions, which reveal this kind of light source has potential application for quantum metrology.

https://doi.org/10.1364/PRJ.386557

1. INTRODUCTION

Benefiting from its narrow bandwidth, paired photons generated from a cold atomic ensemble via four-wave mixing exhibit unique advantages for applications in quantum optics and quantum information research [1–4]. In particular, paired photons produced from three-level or four-level cold atomic ensembles show a strong nonclassical character with a notable violation of the Cauchy–Schwartz inequality [2,5]. However, on one hand, the generation rate of photon pairs strongly depends on the optical depth of the atomic cloud and the pump laser intensity, and thus the stability of experimental conditions is critical when a stable quantum light source is required. On the other hand, to maintain the desired quantum characteristics of the photon pairs, the photon generation rate is typically set at a low level. Although correlated photons also can be generated from a two-level atomic system via four-wave mixing with a generation rate orders of magnitude higher than those in three-level or four-level systems [6,7], strong Rayleigh scattering is usually inevitable and as such, this photon source is typically unacceptable for practical applications. In this investigation, we experimentally determined that even with higher Rayleigh scattering background, the quantum nature of this type of source indicates that it can be effectively utilized in two-photon interference experiments. Surprisingly, the coincidence count of photons generated via Rayleigh scattering with a large time delay provides a reference that can be used to calibrate the normalized second-order correlation function, which is robust under perturbed experimental conditions.

In this report, we experimentally demonstrate the utility of the mixed light field generated from a two-level atomic ensemble by using Hong–Ou–Mandel (HOM) and Hanbury Brown–Twiss (HBT) interferometers [8–11]. It is well-known that the HOM effect is a two-photon interference phenomenon without a classical analog. For photons generated from four-wave mixing and Rayleigh scattering, anticorrelation was observed after they passed through the beam splitter (BS) in the HOM interferometer. In addition, the case of two incident photons with orthogonal polarization was investigated. Moreover, the autocorrelation of photons from one out-port of the HOM instrument was measured by using an HBT device [12,13]. All the observed experimental results agree with our analysis. Finally, we discuss the potential application of this kind of light source in quantum metrology.

2. EXPERIMENTAL SETUP

The experimental configuration used in the investigation is shown in Fig. 1. The setup for paired-photon generation is similar to that described in Ref. [6]. A cold atomic ensemble of ^{87}Rb is initially prepared in a magnetic-optical trap (MOT), and the atoms are subsequently optically pumped to the ground level $|5S_{1/2}, F = 2\rangle$ by switching off the cooling beam while keeping the repump laser on. A linearly polarized

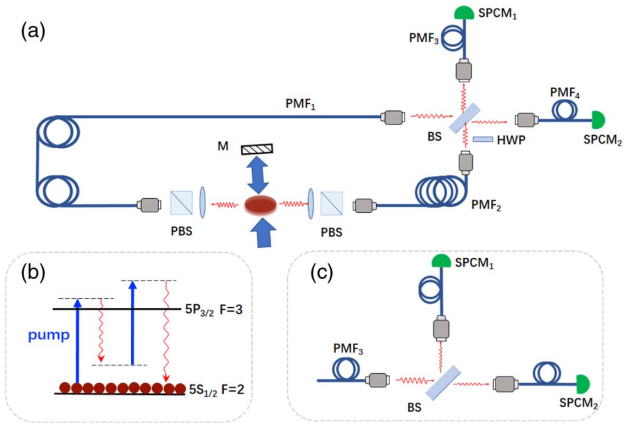

Fig. 1. Sketch of the experimental layout. (a) Generation of paired photons and HOM interferometer; (b) four-wave mixing in a two-level system; (c) measurement of the autocorrelation of photons coming from one out-port of the HOM instrument.

retroreflection-pumped beam with an output power of 1.4 mW and a linewidth of approximately 1 MHz is used to generate photon pairs. The pump beam is collimated with a diameter of 2 mm and completely overlaps with the atomic cloud. The frequency of the pump laser is blue-detuned 54 MHz from the cycle transition $|5S_{1/2}, F = 2\rangle \rightarrow |5P_{3/2}, F' = 3\rangle$. Phase-matched counterpropagating photon pairs are generated via four-wave mixing and are collected by a pair of oppositely positioned polarization-maintaining (PM) single-mode fibers (PMF1 and PMF2). Two polarizers in front of each fiber are set to select incident photons with the same linear polarization. Two photon-counting modules (Perkin-Elmer SPCM-AQR-14) are used to detect the photons, and a time-to-digital converter (Fast Comtec TDC 7888) is used to measure the time correlation between the photon pair. Coincidence counts are measured with a bin width of 1 ns for a range of 512 bins.

When we measure the correlation function of the light field, we connect the ends of the PMF1 and the PMF2 to each photon-counting module directly, while in the HOM experiment, the output photons from the PMF1 and the PMF2 pass through a 50:50 BS; then the superposed beams are incident into two PM fibers (PMF3 and PMF4), which connect to the photon-counting modules. In the HOM interference experiment, we put two polarizers at each out-port of the PMF1 and the PMF2 to ensure the output photons have identical linear polarization. In another experiment, we insert a half-wave plate (HWP) in front of one in-port of the BS; then the polarizations of two photons in front of two in-ports of the BS are perpendicular to each other. We also implement an HBT measurement to obtain the autocorrelation of photons output from one out-port of the HOM interferometer, as shown in Fig. 1(c).

3. RESULTS AND DISCUSSION

A. HOM Interference with the Mixed Light Field

The coincidence count of the light field, as shown in Fig. 2(a), has a damped oscillation with a flat background. The damped oscillation comes from correlated Stokes and anti-Stokes photon pairs, which are generated from the four-wave mixing

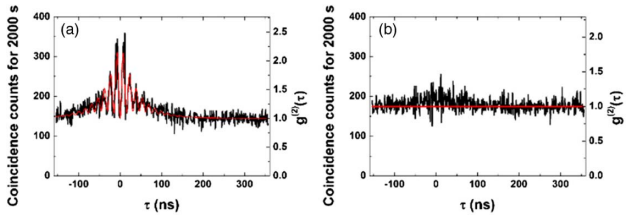

Fig. 2. Experimental results. (a) Coincidence count as a function of the delay between detected photons for paired photon generation in a two-state system; (b) HOM coincidence count.

process in the approximately two-level system. The flat nonzero background is the accidental coincidence from the uncorrelated Rayleigh scatters. Therefore, coincidence counts with a large τ can be used as a reference to normalize the correlation function. The normalized second-order quantum coherence function of the two-photon generation in the two-level system can be expressed as [7]

$$g^{(2)}(\tau) = 1 + \frac{R_{CC}(\tau)}{R_R^2}, \tag{1}$$

where $R_{CC}(\tau)$ is the two-photon coincidence count rate, which is proportional to the grouped constant,

$$R_0 = \left(\frac{\hbar |d_{ge}|^2 |\Omega_1|^2 \omega_1 Q_0 NL}{4\pi\varepsilon_0 c \Delta\Omega_e}\right)^2, \tag{2}$$

and R_R is the linear Rayleigh scattering rate,

$$R_R = \frac{\hbar |d_{eg}|^2 |\Omega_1|^2 \omega_1 NL}{8\varepsilon_0 c \Omega_e^2}. \tag{3}$$

In Eqs. (2) and (3), Q_0 is the parameter of population inversion, which can be approximated as unity. d_{ge} and d_{eg} are dipole matrix elements, $|d_{ge}| = |d_{eg}|$. Ω_1 is the Rabi frequency of the pump beam. ω_1 is the frequency of the pump laser, and Δ is the pump detuning from the atomic transition $|g\rangle \rightarrow |e\rangle$. $\Omega_e = \sqrt{\Delta^2 + \Omega_1^2}$ is the effective Rabi frequency. The product of the atomic density N and the length L is the optical depth of the atomic cloud. It is easy to find: when $|\Delta| > \Omega_1$, the ratio $R_{CC}(\tau)/R_R^2 = g^{(2)}(\tau) - 1$ only slightly depends on the optical depth of the atomic cloud and the intensity of the pump beam, which is effective for reducing any perturbations when the vapor pressure of atoms or the laser power is varied.

For all the data processing performed as part of this investigation, the counts are normalized with the mean value of from $\tau = 200$ ns to $\tau = 357$ ns. The two-photon coincidence counts in Fig. 2(a) are normalized and fitted with the function

$$g^{(2)}(\tau) = 1 + a[e^{-\gamma_1|\tau|} - \cos(\Omega_e\tau)e^{-\gamma_2|\tau|}], \tag{4}$$

where a is the parameter related to the ratio R_0/R_R^2, γ_1 and γ_2 are decay rates that come from the population relaxation of the excitation state and the linewidth of the inhomogeneous-broadened ground state. The spectrum of photons generated from four-wave mixing process has a central component and two sidebands. The oscillation term in Eq. (4) originates from an interference between the central-component correlation and the sideband–sideband correlation. The black lines represent

the experimental data and the red lines come from fitting. The fitted curve agrees well with the experimental data when the fitting parameters $a = 0.7$, $\gamma_1 = 0.02$, $\gamma_2 = 0.033$, and the effective Rabi frequency $\Omega_e = 2\pi \times 65$ MHz are used. Later in this report, we will use the normalized second-order correlation function to investigate the characteristics of the two photon interference processes in the HOM interferometer.

Then we implement the HOM experiment, as we described in the previous section. Figure 2(b) shows the experimental results. It is evident that the coincidence oscillation peaks close to $\tau = 0$ almost vanish. In order to make a quantitative comparison, we define the mean value of $g^{(2)}(\tau) - 1$ from $\tau = -154$ ns to $\tau = 154$ ns as the effective signal S. In the HOM experiment we obtain $S = 0.02 \pm 0.03$, which is nearly zero. Although the paired photons generated from the four-wave mixing process are nondegenerate, the path-exchange symmetry causes the two inputs to be identical, and therefore destructive interference occurs [9,11]. This is easy to be understood by checking the two-photon state

$$|1_1 1_2\rangle = \iint d\omega_s d\omega_{as} \Phi(\omega_s, \omega_{as}) \times [\hat{a}_1^\dagger(\omega_s)\hat{a}_2^\dagger(\omega_{as}) + \hat{a}_1^\dagger(\omega_{as})\hat{a}_2^\dagger(\omega_s)]|0\rangle. \quad (5)$$

Since $\hat{a}_1^\dagger = \frac{1}{\sqrt{2}}(\hat{a}_3^\dagger + \hat{a}_4^\dagger)$ and $\hat{a}_2^\dagger = \frac{1}{\sqrt{2}}(\hat{a}_3^\dagger - \hat{a}_4^\dagger)$, we have

$$|1_1 1_2\rangle = \iint d\omega_s d\omega_{as} \Phi(\omega_s, \omega_{as}) \times [\hat{a}_3^+(\omega_s)\hat{a}_3^+(\omega_{as}) - \hat{a}_4^+(\omega_s)\hat{a}_4^+(\omega_{as})]|0\rangle. \quad (6)$$

Therefore, both two photons appear either in one or another out-port.

We must point out that the destructive two-photon interference occurred not only for paired photons generated from the four-wave mixing process, but also for Rayleigh scatters. If one in-port of the BS in Fig. 1(a) is blocked, the device becomes an HBT interferometer [12]. The coincidence counts of photons from the two out-ports of the BS will yield an autocorrelation function of Rayleigh scatters given as [13]

$$g^{(2)}(\tau) = 1 + e^{-\gamma|\tau|}. \quad (7)$$

This function is represented by a broadened peak with a Lorentzian line shape in the coincidence count data. When both in-ports are open, the broadened coincidence peak will vanish due to the destructive interference. The flat coincidence counts in Fig. 2(b) are the result of destructive two-photon interference for both the case of paired photons and Rayleigh scatters.

We demonstrate the destructive two-photon interference of Rayleigh scatters in the experiment. A blocker is placed before the mirror of the setup so the pump beam is now a traveling wave. The collected counterpropagating photons do not satisfy the phase-matching condition of the four-wave mixing process, and they are Rayleigh scatters from the atomic ensemble. First, we directly measure the coincidence counts of Rayleigh scatters output from the PMF1 and the PMF2. As shown in Fig. 3(a), the coincidence count is flat for all the delay time τ, since there is no correlation between Rayleigh scattered photons from the atomic ensemble under the experimental configuration. Then all the connection of fibers in Fig. 1(a) is resumed, but the

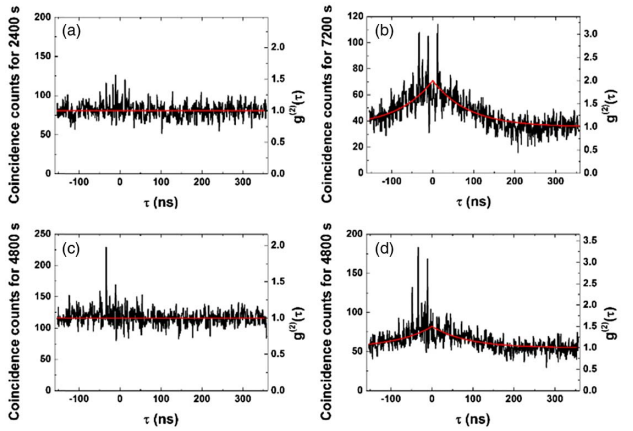

Fig. 3. Experimental results. (a) Coincidence count as a function of the delay between detected photons for Rayleigh scatters; (b) autocorrelation of Rayleigh scatters; (c) HOM coincidence count for Rayleigh scatters; (d) coincidence count for orthogonally polarized photons in the HOM device for Rayleigh scatters.

out-port of the PMF2 is blocked. So, photons only emit from the PMF1 and pass through the BS, which becomes an HBT device for measuring the autocorrelation function of Rayleigh scatters. The normalized coincidence function is shown in Fig. 3(b). The profile is fitted with the function of Eq. (7). We obtain $\gamma = 0.0115$ ns^{-1}, which is the typical laser linewidth instead of the natural linewidth of the atom. Therefore, it is confirmed that the broadened coincidence peak close to $\tau = 0$ is due to Rayleigh scattering. We also measure the autocorrelation function of photons only from PMF2 and get a similar result. Then, the blocker of the fiber is removed, and the HOM experiment is repeated with Rayleigh scatters. It is evident that the broadened peak disappears, as shown in Fig. 3(c).

In Refs. [14–16], anticorrelation in the HOM experiment was observed with a pseudo-thermal light field using a rapidly rotating diffusing ground glass, which is similar to that observed in our investigation. However, in their experiments, the second-order coherence function was obtained by measuring the joint photodetection counting rates versus the optical delay. For each optical delay, a single count was obtained. Therefore, the approach that we adopted to obtain time-resolved correlation counts is not compatible with their experimental setup. Moreover, the long correlation time of the biphotons is critical to our proposed approach.

The behavior of thermal light fields in the HOM device can be depicted from another point of view. Since the density matrix of the system contains all information, we only need to investigate the evolution of the density matrix when thermal light fields pass through the BS. The density matrix of the input Rayleigh scatters can be represented by a positive well-behaved P function. Two classical states of P functions, $P_a(\alpha)$ and $P_b(\alpha)$, are incident on a BS [17,18], and the density matrix of the input states is

$$\rho_{\text{in}} = \int P_a(\alpha_a) P_b(\beta) |\alpha\rangle_a\langle\alpha| \otimes |\beta\rangle_b\langle\beta| d^2\alpha d^2\beta. \quad (8)$$

The BS operator is [17]

$$\hat{B} = \exp\left[\frac{\theta}{2}(\hat{a}^{\dagger}\hat{b}e^{i\phi} - \hat{a}\hat{b}^{\dagger}e^{-i\phi})\right], \tag{9}$$

with the amplitude reflection and transmission coefficients

$$t = \cos\frac{\theta}{2}, \qquad r = \sin\frac{\theta}{2}. \tag{10}$$

ϕ is the phase difference between the reflected and transmitted fields.

The density matrix for the output state is written as

$$\begin{aligned}\rho_{\text{out}} &= \hat{B}\int P_a(\alpha_a)P_b(\beta)|\alpha\rangle_a\langle\alpha| \otimes |\beta\rangle_b\langle\beta|\mathrm{d}^2\alpha\mathrm{d}^2\beta\hat{B}^{+} \\ &= \int P_a(t\gamma - re^{i\phi}\delta)P_b(re^{-i\phi}\gamma + t\delta)|\gamma\rangle_a\langle\gamma| \otimes |\delta\rangle_b\langle\delta|\mathrm{d}^2\gamma\mathrm{d}^2\delta.\end{aligned} \tag{11}$$

For a 0.5:0.5 BS, $t = r = \frac{1}{\sqrt{2}}$. So,

$$\begin{aligned}\rho_{\text{out}} = \int P_a\left(\frac{\gamma - e^{i\phi}\delta}{\sqrt{2}}\right)P_b\left(\frac{e^{-i\phi}\gamma + \delta}{\sqrt{2}}\right)|\gamma\rangle_a\langle\gamma| \\ \otimes |\delta\rangle_b\langle\delta|\mathrm{d}^2\gamma\mathrm{d}^2\delta.\end{aligned} \tag{12}$$

The P function of a thermal field is [19]

$$P(\alpha) = \frac{1}{\pi\langle\hat{n}\rangle}e^{-|\alpha|^2/\langle\hat{n}\rangle}. \tag{13}$$

Here, $\langle\hat{n}\rangle_a = \langle\hat{n}\rangle_b = N$.

Then we have

$$\begin{aligned}P_a\left(\frac{\gamma - e^{i\phi}\delta}{\sqrt{2}}\right)P_b\left(\frac{e^{-i\phi}\gamma + \delta}{\sqrt{2}}\right) &= \frac{1}{\pi^2N^2}\exp\left(-\frac{|\gamma|^2 + |\delta|^2}{N}\right) \\ &= P_a(\gamma)P_b(\delta).\end{aligned} \tag{14}$$

So, $\rho_{\text{out}} = \rho_{\text{in}}$. Since the coincidence count of the input Rayleigh scatters is flat, therefore the coincidence count of the output photons from the BS should also be flat.

B. HOM Experiment with Polarization Distinguishable Photons

Since the HOM effect requires undistinguishable input states, the coincidence peaks will not vanish if the experiment is performed by using paired photons with orthogonal polarization, which can be achieved by inserting an HWP in front of an in-port of the BS. The result is shown in Fig. 4(a), which is significantly different from the profile in Fig. 2(a). A broadened peak is evident at approximately $\tau = 0$ for pulsing oscillation peaks. Next, we will analyze the formation of the line shape.

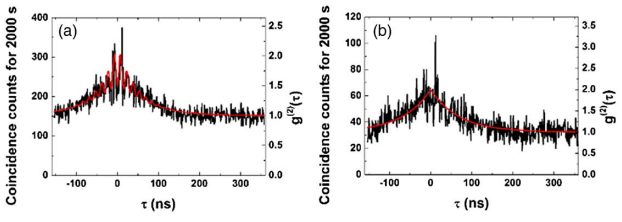

Fig. 4. Experimental results. (a) Coincidence count for orthogonally polarized photons in the HOM device; (b) autocorrelation of photons from one out-port (PMF1) of the light source.

To begin with Eq. (1), we find this expression is valid not only for coincidence count of photon pairs coming from the four-wave mixing process, but also for autocorrelation of Rayleigh scatters. The flat ground that equals to 1 in $g^{(2)}(\tau)$ comes from the accidental coincidence, while the rest $g^{(2)}(\tau) - 1$ indicates the correlation of photons above the random correlation. In the experimental result of Fig. 4(a), $g^{(2)}(\tau) - 1$ is contributed from both the coincidence counts of paired photons and the autocorrelation of Rayleigh scatters.

First, let us check the coincidence counts of paired photons generated from the four-wave mixing process. After inserting the HWP, the two input photons will have orthogonal polarization states. When they pass the BS, there is no two-photon interference. Transmission or reflection of each photon in the photon pair is independent. Therefore, there is a 50% probability that two photons are output from different out-ports and generate coincidence counts. For this reason, R_{CC} should be multiplied by a factor of 0.5 and be compared with the direct coincidence measurement of photon pairs. The linear Rayleigh scattering rate R_R is constant with or without the BS. Therefore, $g^{(2)}(\tau) - 1$ from the paired photons should be multiplied by a factor of 0.5 and compared with the direct coincidence measurement.

Then we check the contribution of the autocorrelation of Rayleigh scatters. The total coincidence count is the intensity sum of two autocorrelation measurements with orthogonally polarized photons. So $R_{CC}(\tau)$ should be multiplied by a factor of 2 and compared with a single input port, while R_R also should be multiplied by a factor of 2 and compared with a single input port. Therefore, it is easy to get $g^{(2)}(\tau) - 1$, which should be multiplied by a factor of 0.5 and compared with the autocorrelation measurement with a single in-port. In Figs. 5(a) and 5(b), we show the contribution of each situation to $g^{(2)}(\tau)$, just as we discussed above.

Above, we assumed the BS and fiber coupling are lossless. However, even taking into account the balanced loss due to BS and fiber coupling, this deduction is still valid. Now we get the conclusion that the profile of $g^{(2)}(\tau) - 1$ in the experiment with orthogonal polarization states should be the superposition of the two component states that originate from paired photons and Rayleigh scatters multiplied by a factor of 0.5, respectively.

To evaluate the aforementioned results and assertions, first, we perform an experiment with only Rayleigh scatters. We put a blocker in front of the mirror to ensure a traveling-wave pump beam. Then we do the HOM experiment with orthogonal polarization Rayleigh scatters. The result is shown as Fig. 3(d), and $S = 0.27 \pm 0.05$. In the autocorrelation measurement of Rayleigh scatter from a single input port, as shown in Fig. 3(b), S is 0.48 ± 0.06. So, in the HOM experiment with orthogonal polarization Rayleigh scatters, $g^{(2)}(\tau) - 1$ is approximately half the value of the autocorrelation measurement of Rayleigh scatter from a single input port.

It is well known that in the weak driving field limit, the resonance fluorescence spectrum is dominated by Rayleigh scattering. However, the spectrum width broadens with an increase of the pump power [13,20–22]. In order to perform the autocorrelation measurements under real experimental conditions, the experiment is repeated with photons generated from a

standing-wave pump beam. The result is shown in Fig. 4(b). The data are fitted using Eq. (7), and a value of $\gamma = 0.0145\ \text{ns}^{-1}$ is obtained. In this case, we get $S = 0.40 \pm 0.05$.

Once all the parameters in Eqs. (4) and (7) are obtained, these equations are multiplied by a factor of 0.5, and their sum is determined. The red line in Fig. 4(a) represents this result, which is in agreement with the experimental data. In the coincidence measurement of paired photons, as shown in Fig. 2(a), we get $S = 0.23 \pm 0.03$, while for input photons with orthogonal polarization, as shown in Fig. 4(a), we obtain $S = 0.30 \pm 0.03$. Within the limit of error, the value is equal to the sum of half the value for the paired photons and half that of the Rayleigh scatters.

C. Autocorrelation of Photons from One Out-Port of the HOM Interferometer

For further demonstration of the availability of this light source, we investigate the following issue. The anticorrelation between the two out-ports of the BS in the HOM experiment reveals that both input photons propagate in the same beam simultaneously [8,23–25], which is also known as the bunching effect. Nevertheless, bunching of photons is hard to confirm by directly measuring the number of photons from one out-port of the HOM interferometer unless we have photon number-resolved detectors [26,27]. Here we consider an alternative way to observe the bunching effect. If we put a BS behind one of the out-ports of the HOM interferometer, as shown in Fig. 1(c), the HBT measurement will give the autocorrelation of photons. The absent correlation peaks should reappear, since the bunched correlated photons have a 50% probability of being detected by different single-photon modules. However, it is also possible that photons coming from the PMF1 and the PMF2, respectively, are injected into the same out-port of the HOM interferometer just by chance. Therefore, the reappearance of the correlation peaks is not enough to confirm the photon bunching effect. By exploiting the background reference of the Rayleigh scatters, the normalized second-order correlation function provides a quantitative determination of the matter. A simple analysis is presented: first, we consider the case of the same polarization. Compared to a direct measurement, the count rate for a single photodetector after the second BS should be multiplied by a factor of 0.5. Therefore, the background coincidence count rate R_R^2 with a large delay time should be multiplied by a factor of 0.25. Then we check the two-photon coincidence count rate, $R_{CC}(\tau)$. If the photon pairs generated from four-wave mixing have the same polarization, the probability that they will be emitted from one of the out-ports is halved. Therefore, the photon pairs that are output from the chosen fiber should be multiplied by a factor of 0.5. The paired photons then meet the second BS, and they have a 50% probability of producing coincidence counts. Another 50% probability is that the pair will enter the same detector without generating coincidence counts. Therefore, $R_{CC}(\tau)$ should also be multiplied by a factor of 0.25.

We arrive at the following conclusion: for entangled photon pairs, $g^{(2)}(\tau) - 1$ after the second BS should be the same as that of the direct measurement of the coincidence count. The broadened peak due to the Rayleigh scatters should also be the same as that due to direct autocorrelation measurements.

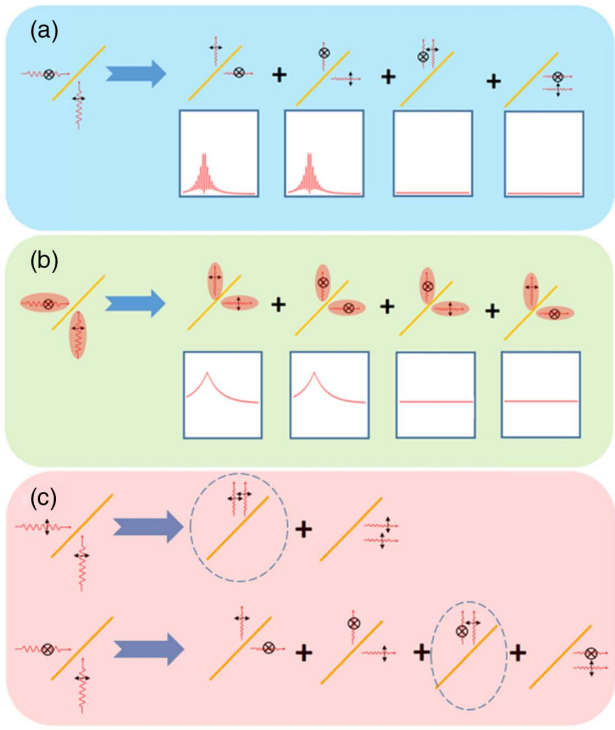

Fig. 5. Effect of intensity superposition for orthogonal polarization. (a) Paired photons and (b) Rayleigh scatters. The red lines in square frames represent contributions of each case to $g^{(2)}(\tau)$. (c) For input paired photons with the same polarization, the probability of two photons being injected into PMF3 simultaneously is 50%, while for orthogonal polarization photons, the probability is 25%.

This is because the field of Rayleigh scattering is a thermal field, and it does not change after passing through a BS, which has been proved in Section 3.A. Therefore, for photons with the same polarization, $g^{(2)}(\tau) - 1$ should be the sum of the direct coincidence measurement of paired photons and the direct autocorrelation measurement of the Rayleigh scatters. However, for the orthogonally polarized input, all counts are the result of intensity superposition instead of amplitude superposition. In Fig. 5(c), we show the probability of orthogonal polarization photons being injected into PMF3 simultaneously is only half of that of the same polarization photons. Using an analysis similar to that used for Fig. 4(a), it is easy to see for orthogonally polarized photons, $g^{(2)}(\tau) - 1$ should be the combination of half the correlation of entangled photon pairs and half the autocorrelation of Rayleigh scatters.

The experimental result is shown in Fig. 6. It is observed in Fig. 6(a) that the profile of the correlation count is in agreement with the red line, which represents the superposition of the components that originate from the four-wave mixing and the Rayleigh scatters. In Fig. 6(b), the data are poor, but a similar trend with the red line is still observed. It should be emphasized that there are no free-fitting parameters in the red lines in Figs. 6(a) and 6(b). All parameters come from the red fitting lines in Figs. 2(a) and 4(b). Then we make a quantitative comparison between our analysis and experimental results. We find $S = 0.60 \pm 0.05$ in Fig. 6(a). In comparison

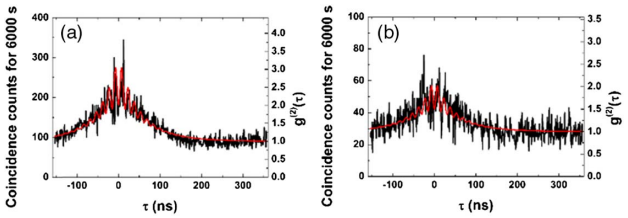

Fig. 6. Experimental results. (a) Autocorrelation function of the photons from one out-port of the HOM interferometer; (b) autocorrelation function of the photons from one out-port of the HOM device with orthogonally polarized photons.

with the values obtained from Figs. 2(a) and 4(b), it is determined that this value is equal to the sum of the value for the paired photons and that of the Rayleigh scatters, within the limit of experimental error, while in the case of the orthogonal polarization $S = 0.32 \pm 0.06$, which is approximately half that of the previous, which is in agreement with the aforementioned analysis.

4. OUTLOOK AND CONCLUSION

In the HOM experiment described in Section 3.A, both the entangled photon pairs and Rayleigh scatters exhibit the destructive two-photon interference. However, it should be emphasized that when they pass through the BS, their behavior is different. The state of the entangled photon pairs changes, while that of the Rayleigh scatters does not change, which is manifested from the mathematical expression in Section 3.A. This difference could be important in quantum metrology with two-photon interferometry [28,29]. For instance, if a Mach–Zehnder (MZ) interferometer with two 0.5:0.5 BSs is built, and the coincidence count from two out-ports is measured, damped oscillations will be observed that are attributable to entangled photon pairs, and the amplitude of the oscillations will vary with the difference in the optical path length. Meanwhile, balanced input of the Rayleigh scatters results in a constant flat background without dependence on the difference in the optical path length. So, we can extract $g^{(2)}(\tau) - 1$ as the interference signal. Compared with the entangled photon pairs or thermal light, which were already used in two-photon interference [30–35], the mixed light field generated from a two-level atomic ensemble provides a self-calibrated output signal. Even under perturbed experimental conditions, a stable two-photon interference signal is still obtained by measuring the normalized second-order correlation function. Recently, we got preliminary data of two-photon interference in an MZ interferometer with the mixed light field. More details will be discussed in future articles.

In conclusion, the utility of the mixed light field generated in a two-level atomic ensemble via four-wave mixing and Rayleigh scattering has been experimentally demonstrated. The background coincidence count with a large delay time provides a reference for obtaining the normalized second-order correlation function, which is insensitive to fluctuation of the experimental conditions. The HOM interference signal, the effect of distinguishability for orthogonally polarized photon pairs, and the bunching effect of photons are observed, which agree well with theoretical predictions. These experiments and analysis manifest that this kind of light source has potential value in quantum metrology.

Funding. National Natural Science Foundation of China (11674338, U1730126, 11804105, 11547024).

Acknowledgment. We thank R. Folman, J. Qian, X. B. Wang, and Y. S. Zhang for helpful discussions.

Disclosures. The authors declare no conflicts of interest.

REFERENCES

1. V. Balić, D. A. Braje, P. Kolchin, G. Yin, and S. E. Harris, "Generation of paired photons with controllable waveforms," Phys. Rev. Lett. **94**, 183601 (2005).
2. P. Kolchin, S. Du, C. Belthangady, G. Yin, and S. E. Harris, "Generation of narrow-bandwidth paired photons: use of a single driving laser," Phys. Rev. Lett. **97**, 113602 (2006).
3. S. Du, C. Belthangady, P. Kolchin, G. Y. Yin, and S. E. Harris, "Observation of optical precursors at the biphoton level," Opt. Lett. **33**, 2149–2151 (2008).
4. Z. Han, P. Qian, L. Zhou, J. F. Chen, and W. Zhang, "Coherence time limit of the biphotons generated in a dense cold atom cloud," Sci. Rep. **5**, 9126 (2015).
5. L. Zhao, X. Guo, C. Liu, Y. Sun, M. M. T. Loy, and S. Du, "Photon pairs with coherence time exceeding 1 μs," Optica **1**, 84–88 (2014).
6. S. Du, J. Wen, M. H. Rubin, and G. Yin, "Four-wave mixing and biphoton generation in a two-level system," Phys. Rev. Lett. **98**, 053601 (2007).
7. J. Wen, S. Du, and M. H. Rubin, "Biphoton generation in a two-level atomic ensemble," Phys. Rev. A **75**, 033809 (2007).
8. C. K. Hong, Z. Y. Ou, and L. Mandel, "Measurement of subpicosecond time intervals between two photons by interference," Phys. Rev. Lett. **59**, 2044–2046 (1987).
9. C. Liu, J. F. Chen, S. Zhang, S. Zhou, Y. H. Kim, M. M. T. Loy, G. K. L. Wong, and S. Du, "Two-photon interferences with degenerate and nondegenerate paired photons," Phys. Rev. A **85**, 021803 (2012).
10. H. Kim, S. M. Lee, O. Kwon, and H. S. Moon, "Observation of two-photon interference effect with a single non-photon-number resolving detector," Opt. Lett. **42**, 2443–2446 (2017).
11. Y. Zhou, J. B. Liu, H. B. Zheng, H. Chen, F. L. Li, and Z. Xu, "Second-order interference of two independent photons with different spectra," Chin. Phys. B **28**, 104205 (2019).
12. R. Hanbury Brown and R. Q. Twiss, "Correlation between photons in two coherent beams of light," Nature **177**, 27–29 (1956).
13. M. O. Scully and M. S. Zubairy, "Field-field and photon-photon interferometry," in *Quantum Optics* (Cambridge University, 1997), Chap. 4.
14. H. Chen, T. Peng, S. Karmakar, Z. Xie, and Y. Shih, "Observation of anticorrelation in incoherent thermal light fields," Phys. Rev. A **84**, 033835 (2011).
15. H. Chen, T. Peng, S. Karmakar, and Y. Shih, "Simulation of Bell states with incoherent thermal light," New J. Phys. **13**, 083018 (2011).
16. H. Chen, T. Peng, and Y. Shih, "100% correlation of chaotic thermal light," Phys. Rev. A **88**, 023808 (2013).
17. M. S. Kim, W. Son, V. Bužek, and P. L. Knight, "Entanglement by a beam splitter: nonclassicality as a prerequisite for entanglement," Phys. Rev. A **65**, 032323 (2002).
18. X. B. Wang, "Theorem for the beam-splitter entangler," Phys. Rev. A **66**, 024303 (2002).
19. W. P. Schleich, "Phase space functions," in *Quantum Optics in Phase Space* (Wiley, 2001), Chap. 12.
20. B. R. Mollow, "Power spectrum of light scattered by two-level systems," Phys. Rev. **188**, 1969–1975 (1969).

21. H. J. Kimble and L. Mandel, "Theory of resonance fluorescence," Phys. Rev. A **13**, 2123–2144 (1976).
22. F. Y. Wu, R. E. Grove, and S. Ezekiel, "Investigation of the spectrum of resonance fluorescence induced by a monochromatic field," Phys. Rev. Lett. **35**, 1426–1429 (1975).
23. Y. H. Shih and C. O. Alley, "New type of Einstein-Podolsky-Rosen-Bohm experiment using pairs of light quanta produced by optical parametric down conversion," Phys. Rev. Lett. **61**, 2921–2924 (1988).
24. W. A. T. Nogueira, S. P. Walborn, S. Pádua, and C. H. Monken, "Generation of a two-photon singlet beam," Phys. Rev. Lett. **92**, 043602 (2004).
25. S. Restuccia, M. Toroš, G. M. Gibson, H. Ulbricht, D. Faccio, and M. J. Padgett, "Photon bunching in a rotating reference frame," Phys. Rev. Lett. **123**, 110401 (2019).
26. A. Divochiy, F. Marsili, D. Bitauld, A. Gaggero, R. Leoni, F. Mattioli, A. Korneev, V. Seleznev, N. Kaurova, O. Minaeva, G. Gol'tsman, K. G. Lagoudakis, M. Benkhaoul, F. Lévy, and A. Fiore, "Superconducting nanowire photon-number-resolving detector at telecommunication wavelengths," Nat. Photonics **2**, 302–306 (2008).
27. Z. L. Zhou, S. Jahanmirinejad, F. Mattioli, D. Sahin, G. Frucci, A. Gaggero, R. Leoni, and A. Fiore, "Superconducting series nanowire detector counting up to twelve photons," Opt. Express **22**, 3475–3489 (2014).
28. V. Giovannetti, S. Lloyd, and L. Maccone, "Advances in quantum metrology," Nat. Photonics **5**, 222–229 (2011).
29. D. N. Klyshko, "Quantum optics: quantum, classical, and metaphysical aspects," Physics-Uspekhi **37**, 1097–1124 (1994).
30. J. G. Rarity, P. R. Tapster, E. Jakeman, T. Larchuk, R. A. Campos, M. C. Teich, and B. E. A. Saleh, "Two-photon interference in a Mach-Zehnder interferometer," Phys. Rev. Lett. **65**, 1348–1351 (1990).
31. R. A. Campos, B. E. A. Saleh, and M. C. Teich, "Fourth-order interference of joint single-photon wave packets in lossless optical systems," Phys. Rev. A **42**, 4127–4137 (1990).
32. T. S. Kim, H. O. Kim, J. H. Ko, and G. D. Park, "Two-photon interference experiment in a Mach-Zehnder interferometer," J. Opt. Soc. Korea **7**, 113–118 (2003).
33. D. Z. Cao, C. Ren, J. Y. Ni, Y. Zhang, S. H. Zhang, and K. G. Wang, "Flexible two-photon interference fringes with thermal light," Sci. Rep. **7**, 1930 (2017).
34. J. B. Liu, H. Chen, Y. Zhou, H. B. Zheng, F. L. Li, and Z. Xu, "Second-order fermionic interference with independent photons," J. Opt. Soc. Am. B **34**, 1215–1222 (2017).
35. Z. Y. Zhou, S. K. Liu, S. L. Liu, Y. H. Li, Y. Li, C. Yang, Z. H. Xu, G. C. Guo, and B.-S. Shi, "Revealing the behavior of photons in a birefringent interferometer," Phys. Rev. Lett. **120**, 263601 (2018).